Eddy diffusivity from hydromagnetic Taylor-Couette flow experiments

Marcus Gellert* and Günther Rüdiger†
Astrophysikalisches Institut Potsdam, An der Sternwarte 16, D-14482 Potsdam, Germany
(Received 30 January 2009; revised manuscript received 27 September 2009; published 22 October 2009)

The stability problem of hydromagnetic Taylor-Couette flows with toroidal magnetic fields is considered for various magnetic Prandtl numbers. Only the most uniform (but not current-free) field has been treated. For high enough Hartmann numbers, the toroidal field is always unstable due to the magnetic kink-type instability, which is stabilized by rigid basic rotation. The axial electric current, which drives the instability, is reduced by the electromotive force induced by the instability itself. Numerical simulations show that this electromotive force only depends on the molecular magnetic diffusivity rather than the viscosity. The resulting eddy diffusivity should be on the order of the molecular diffusivity for all the considered magnetic Prandtl numbers. If this is true also for very small magnetic Prandtl numbers (not possible to simulate) then one can use this effect to measure the eddy diffusivity η_T in a laboratory. In a sodium experiment (without rotation), a detectable potential difference of ~ 16 mV between top and bottom will result for a container of 1 m length and a gap width of 10 cm.

DOI: 10.1103/PhysRevE.80.046314 PACS number(s): 47.20.Ft, 47.65.−d

I. INTRODUCTION

Strong enough toroidal fields, which are not current free, become unstable due to the Tayler instability (TI [1–3]). Because the source of the energy is the electric current, this (mainly nonaxisymmetric) instability can exist even without any rotation. There is no laboratory experiment for this basic instability so far, and even the numerical simulations of TI are very rare [4,5]. We shall demonstrate in the present paper for Taylor-Couette (TC) flows of fluids with various magnetic Prandtl numbers how the TI works and how it interacts with rotation, which can be nonuniform. The theoretical results are used to suggest experiments for measuring the effective diffusivity via a TI-induced reduction in the applied electromotive force (EMF).

The knowledge of the magnetic turbulent diffusivity is basic for many applications in fluid dynamics. Very often we have only limited informations about its value. Only a very small number of experiments have been done in laboratories (see [6–8]). The same is true for the viscosity, which should be measurable with the same experiment so that finally the modified magnetic Prandtl number becomes known from one and the same instability experiment.

Consider a laminar hydromagnetic TC flow with $\boldsymbol{U}$ as the velocity, $\boldsymbol{B}$ as the magnetic background field, ν as the microscopic viscosity, and η as the microscopic magnetic diffusivity. The basic state in cylindrical geometry is $U_R = U_z = B_R = B_z = 0$ and

$$U_\phi = R\Omega = a_\Omega R + \frac{b_\Omega}{R}, \quad B_\phi = a_B R + \frac{b_B}{R}. \tag{1}$$

Let

$$\hat{\eta} = \frac{R_{\rm in}}{R_{\rm out}}, \quad \mu_\Omega = \frac{\Omega_{\rm out}}{\Omega_{\rm in}}, \quad \mu_B = \frac{B_{\rm out}}{B_{\rm in}} \tag{2}$$

and $R_{\rm in}$ and $R_{\rm out}$ be the radii of the inner and outer cylinders, $\Omega_{\rm in}$ and $\Omega_{\rm out}$ their rotation rates, and $B_{\rm in}$ and $B_{\rm out}$ their azimuthal magnetic fields at the inner and outer cylinders. In particular, a field of the form b_B/R is generated by an axial current only through the inner region $R < R_{\rm in}$, whereas a field of the form $a_B R$ is generated by a uniform axial current through the entire region $R < R_{\rm out}$ including the fluid.

The magnetic Prandtl number Pm, the Reynolds number Re, and the Hartmann number Ha,

$$\mathrm{Pm} = \frac{\nu}{\eta}, \quad \mathrm{Re} = \frac{\Omega_{\rm in} D^2}{\nu}, \quad \mathrm{Ha} = \frac{B_{\rm in} D}{\sqrt{\mu_0 \rho \nu \eta}}, \tag{3}$$

are the basic parameters of the problem, where $D = R_{\rm out} - R_{\rm in}$.

The stability maps are the result of a linear theory for both axisymmetric perturbation modes ($m=0$) and nonaxisymmetric perturbation modes ($m=1$). Michael [9] and Velikhov [10] considered axisymmetric disturbances and derived for $\Omega = 0$ the stability criterion

$$\frac{d}{dR}\left(\frac{B_\phi}{R}\right)^2 < 0 \tag{4}$$

for magnetic instabilities. Tayler [3] included nonaxisymmetric disturbances and revealed for an ideal fluid the relation

$$\frac{d}{dR}(RB_\phi^2) < 0 \tag{5}$$

as necessary and sufficient condition for stability. The linearized MHD equations for a TC flow $\boldsymbol{U}$ subject to a magnetic background field $\boldsymbol{B}$ for the small disturbances $\boldsymbol{u}' = \boldsymbol{u} - \boldsymbol{U}$ and $\boldsymbol{b}' = \boldsymbol{b} - \boldsymbol{B}$ are

$$\frac{\partial \boldsymbol{u}'}{\partial t} + (\boldsymbol{u}'\nabla)\boldsymbol{U} + (\boldsymbol{U}\nabla)\boldsymbol{u}' = -\nabla(p'/\rho) + \nu\Delta\boldsymbol{u}' + \mathrm{curl}\boldsymbol{B} \times \boldsymbol{b}' + \mathrm{curl}\boldsymbol{b}' \times \boldsymbol{B},$$

*mgellert@aip.de
†gruediger@aip.de

 ©2009 The American Physical Society

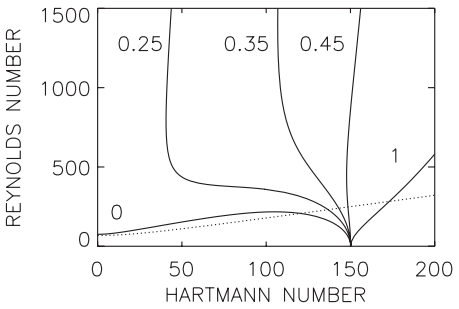

FIG. 1. Conducting walls: the marginal stability curves for $m=0$ (dotted, here only existing for $\mu_\Omega=0$) and $m=1$ (solid). μ_Ω as indicated. $\mu_\Omega=0$ (resting outer cylinder), $\mu_\Omega=0.25$ (Rayleigh limit), $\mu_\Omega=0.35$, $\mu_\Omega=0.45$, and $\mu_\Omega=1$ (rigid rotation). $\mathrm{Pm}=10^{-5}$, $\mu_B=1$, and $\hat{\eta}=0.5$.

$$\frac{\partial \boldsymbol{b}'}{\partial t} = \eta \Delta \boldsymbol{b}' + \mathrm{curl}(\boldsymbol{u}' \times \boldsymbol{B} + \boldsymbol{U} \times \boldsymbol{b}'), \tag{6}$$

with $\mathrm{div}\boldsymbol{u}'=\mathrm{div}\boldsymbol{b}'=0$. p' are the pressure fluctuations. Equations (6) will be normalized with D as the unit of length, η/D as the unit of velocity. B_{in} is the unit of the magnetic fields. Frequencies including the rotation rate Ω are normalized with Ω_{in}.

For the velocity, the hydrodynamic boundary conditions at the walls are assumed as no slip ($\boldsymbol{u}'=0$). At the conducting walls, the radial component of the field and the tangential components of the current must vanish so that $db'_\phi/dR + b'_\phi/R = b'_R = 0$ at both R_{in} and R_{out}.

While our linear stability code also works for the very small Pm of liquid metals, the minimum microscopic Pm, which can be handled with the nonlinear code, is 10^{-2}. The numerical simulations cannot yet deal with the very small magnetic Prandtl numbers of the conducting fluids used in the MHD laboratory ($\mathrm{Pm} \lesssim 10^{-5}$). Some of our results, therefore, can only be obtained with extrapolations.

II. INSTABILITY MAPS FOR LIQUID SODIUM

In order to demonstrate the realizations of the magnetic instability, we now present maps of marginal instability for various magnetic profiles and different rotation laws in liquid sodium ($\mathrm{Pm}=10^{-5}$). The nonlinear simulations presented below leading to calculations of the eddy diffusivity are done only for the most simple realization of a nearly constant field, i.e., $\mu_B=1$. The container is at rest or rotates differentially with resting ($\mu_\Omega=0$) or corotating ($\mu_\Omega=0.35$) outer cylinder. For an aspect ratio of $\hat{\eta}=0.5$, the latter value mimics the Kepler rotation law.

A. Resting outer cylinder

Figure 1 also shows the results for $\mu_B=1$ and for resting outer cylinder, so that for vanishing magnetic field the rotation law is centrifugally unstable if $\mathrm{Re}>68$. We know that for certain μ_B, the $m=1$ mode is unstable while the $m=0$ mode is stable [3,14]. The values $\mu_B=1$ and $\mu_\Omega=0$ in Fig. 1 are a good example. There is always a crossover point at which the most unstable mode changes from $m=0$ (dotted) to $m=1$ (solid). Note also that for $\mu_\Omega=0$, the critical Reynolds numbers of both modes steadily increase for low Ha, while the $m=1$ mode is suddenly decreasing for a sufficiently strong magnetic field. Hence, weak fields initially can stabilize the flow and stronger fields eventually decay via a nonaxisymmetric instability mode. Beyond $\mathrm{Ha}=150$ the field is unstable for all Re, i.e., with and without rotation. Except for the almost current-free profile $\mu_B=0$, all other μ_B are characterized by a critical Hartmann number beyond which the toroidal magnetic fields cannot be stabilized by rotation ([11]). Let $\mathrm{Ha}^{(0)}$ and $\mathrm{Ha}^{(1)}$ denote these critical Hartmann numbers for the modes with $m=0$ and $m=1$.

B. Flat rotation laws

The situation is more complicated if the rotation law is so flat that it is hydrodynamically stable. Then there is no critical Reynolds number at the vertical axis. Instabilities are always due to the magnetic fields but the form of the rotation law strongly influences the instability map. In the following for the most homogeneous magnetic profile with $\mu_B=1$, this influence is demonstrated. Figure 1 gives the curves of marginal stability for $\mu_\Omega=0$, $\mu_\Omega=0.25$ (Rayleigh limit), $\mu_\Omega=0.35$ (Kepler law), $\mu_\Omega=0.45$, and $\mu_\Omega=1$ (rigid rotation). One finds the TI more and more *stabilized* by the basic rotation. Note the massive quenching of the TI by rigid rotation (see [12]). Even a rather slow but rigid rotation stabilizes the toroidal field for $\mathrm{Ha} \geq 150$. Rigidly, rotating containers can keep much stronger fields as stable than those without solid-body rotation.

The rotational stabilization is modified by nonrigid rotation. At the Rayleigh limit ($\Omega \propto R^{-2}$), even a slow rotation destabilizes the system while it is stabilized again for fast rotation. Thus, fast rotation stabilizes and slow rotation destabilizes. At medium Hartmann numbers of (say) 50, one finds for increasing rotation rate at the Rayleigh limit the regimes *stable-unstable-stable*. The critical Reynolds numbers of this sequence are ~ 300 and ~ 1800, which easily can be realized in the laboratory. A similar situation holds for the (quasi-)Kepler rotation law with $\mu_\Omega=0.35$, while for rotation laws with $\mu_\Omega \gtrsim 0.45$ only the rotational stabilization can be observed. In all cases, the reason for the rotational stabilization is the incompatibility of differential rotation and nonaxisymmetric magnetic fields.

This, of course, is also true if the magnetic field is current free ($B_\phi \propto 1/R$ [13]). Fast rotation always suppresses the magnetic instability but differential rotation with negative shear is even able to destabilize the system—if it is not too strong and if the rotation is not too fast (see Fig. 1).

C. Electric currents

For experiments, the available electric currents must not be too strong. Currents of $\simeq 15$ kA can be considered as an upper limit. In order to translate the critical Hartman numbers into amplitudes of electrical currents, we apply our results to liquid sodium with density of 0.92 $\mathrm{g/cm^3}$, a microscopic magnetic diffusivity of 810 $\mathrm{cm^2/s}$, and a magnetic Prandtl number of 10^{-5}. Alternatively, for an alloy of gallium-indium tin, the necessary currents are stronger by a

TABLE I. Characteristic Hartmann numbers and electric currents for a sodium container ($\hat{\eta}=0.5$) with conducting walls. The experiment with the almost uniform field $\mu_B=1$ is indicated in bold.

μ_B	$\mathrm{Ha}^{(0)}$	$\mathrm{Ha}^{(1)}$	I_{axis} (kA)	I_{fluid} (kA)
−2	19.8	24.8	0.807	−4.04
−1	59.3	63.7	2.42	−7.25
1	∞	**151**	**6.16**	**6.16**
2	∞	35.3	1.44	4.32

factor of 3.15. A wider gap possesses lower critical Hartmann numbers and, thus, lower currents are needed for experiments ([11]).

Let I_{axis} be the axial current inside the inner cylinder and I_{fluid} be the axial current through the fluid (i.e., between inner and outer cylinder). Then the toroidal field amplitudes at the inner and outer cylinders are

$$B_{\mathrm{in}}=\frac{I_{\mathrm{axis}}}{5R_{\mathrm{in}}},\quad B_{\mathrm{out}}=\frac{I_{\mathrm{axis}}+I_{\mathrm{fluid}}}{5R_{\mathrm{out}}},\tag{7}$$

measured in cm, Gauss, and Ampere. Expressing I_{axis} and I_{fluid} in terms of our dimensionless parameters, one finds

$$I_{\mathrm{axis}}=5\sqrt{\mu_0\rho\nu\eta}\mathrm{Ha},\quad I_{\mathrm{fluid}}=(2\mu_B-1)I_{\mathrm{axis}}.\tag{8}$$

Note that for $\mu_B=1$, both the currents are equal, which constellation is marked in bold in Table I. The table gives the electric currents needed to reach the minimum of $\mathrm{Ha}^{(0)}$ and $\mathrm{Ha}^{(1)}$ for $\hat{\eta}=0.5$, μ_B ranging from −2 to 2 in each case. For large $|\mu_B|$, the currents I_{fluid} approach constant values.

We favor an experiment with almost uniform field $\mu_B=1$. For a container with a gap of $\hat{\eta}=0.5$, parallel currents of 6.16 kA are necessary along the axis and through the fluid. The experiment does not possess the weakest electric currents, but both the currents are parallel and have the same amplitudes. Figure 1 shows that in this case a crossing point exists, where the axisymmetric mode has the same characteristic Reynolds number and Hartmann number as the nonaxisymmetric mode with $m=1$.

III. EDDY DIFFUSIVITY

It is known that the electric conductivity is reduced by random flows in a conducting fluid or—in other words—that the fluctuations enhance the magnetic diffusivity. Such a turbulence-induced magnetic diffusivity is often termed as the turbulent diffusivity. The diffusivity is also enhanced if the flow pattern is quasistationary and the averaging procedure concerns a coordinate, where the pattern is small scaled. The Reynolds rules are the main conditions to be fulfilled. In our simulations, eddies are concerned averaged over the azimuth rather than turbulence with a flat mode spectrum. We shall call, therefore, the magnetic diffusivity due to the Tayler instability as an "eddy diffusivity."

In the MHD regime, the eddy diffusivity is a simpler quantity than the corresponding eddy viscosity by which angular momentum is transported. The total eddy viscosity is formed by both a Reynolds stress part and a Maxwell stress part. This is not the case for the turbulent diffusivity. In the kinetic quasilinear approximation for a turbulence field with a correlation time τ_{corr},

$$\nu_{\mathrm{T}}\simeq\left(\frac{2}{15}\langle u'^2\rangle+\frac{1}{3}\frac{\langle b'^2\rangle}{\mu_0\rho}\right)\tau_{\mathrm{corr}}\tag{9}$$

results for the eddy viscosity but the much simpler expression

$$\eta_{\mathrm{T}}\simeq\frac{\tau_{\mathrm{corr}}}{3}\langle u'^2\rangle\tag{10}$$

results for the eddy diffusivity [15]. The magnetic fluctuations do *not* contribute to the magnetic diffusivity. This basic difference between the diffusion coefficients is not proven so far by any experiment.

The results (9) and (10) suggest that in (nonrotating) turbulent-magnetized fluids, the effective magnetic Prandtl number always exceeds the minimum value 0.4, which was indeed confirmed by numerical simulations for driven MHD turbulence with Pm of order unity [16].

The knowledge of the turbulent magnetic Prandtl number is of extraordinary meaning in fluid mechanics and geo/astrophysics. For its experimental realization, one has to measure both quantities simultaneously in one and the same experiment. In this paper, we start to present an MHD experiment only for the measurement of η_{T}. Later calculations will also concern the corresponding eddy viscosity ν_{T}.

The nonaxisymmetric components of both flow and field may be used in the following as the "fluctuations," while the axisymmetric components are considered as the background quantities. Then the averaging procedure is simply the integration over the azimuth ϕ.

Because there is no α effect without stratification, it is standard to express the turbulence-induced EMF as

$$\mathcal{E}=\langle\boldsymbol{u}'\times\boldsymbol{b}'\rangle=-\eta_{\mathrm{T}}\mathrm{curl}\boldsymbol{B}.\tag{11}$$

Here the eddy diffusivity η_{T} is considered as a scalar, which must be positive. Higher-order correlations can be neglected because of the small size of fluctuations compared to the mean field. In cylindrical geometry, the mean current curl$\boldsymbol{B}$ has only a z component. Hence, along the axis

$$\mathcal{E}_z=-\eta_{\mathrm{T}}\mathrm{curl}_z\boldsymbol{B}.\tag{12}$$

Indeed, the nonlinear simulations provide the amplitudes of the other components as less than 10% of the amplitude of $\mathcal{E}_z$. After averaging, the mean values are below 1%.

After Table I for $\mu_B=1$, the current through the fluid is positive. Then only for *negative* $\mathcal{E}_z$ the η_{T} results as positive. In the following nonlinear simulations for $\mu_B=1$, the $\mathcal{E}_z$ indeed proves to be negative.

IV. NONLINEAR SIMULATIONS

Absolute values for $\mathcal{E}_z$ can only be computed with nonlinear simulations. The smallest possible magnetic Prandtl number of our code yielding robust results is 0.01. In the present

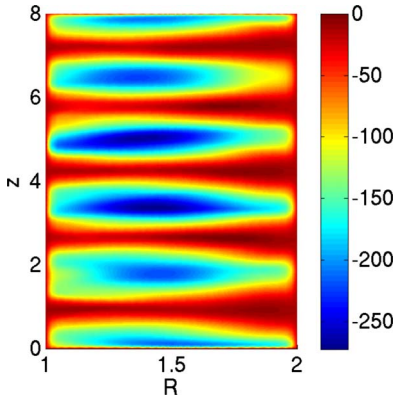

FIG. 2. (Color online) The normalized axial EMF (12) in the container. Everywhere, the correlations are negative. $\mu_B=1$, Ha $=200$, Re$=500$, and Pm$=0.01$.

paper, the results without and with rotation are reported but only for the fixed value of Ha$=200$. The used Fourier spectral element code used has been described earlier in detail [17]. It solves the MHD equations for an incompressible, viscous, and electrically conducting fluid. Velocity and magnetic field are expanded in Fourier modes in azimuthal direction, and the resulting meridional problems are solved using a Legendre spectral element method (see [18]). Either $M=8$ or $M=16$ Fourier modes are used, two or three elements in radius and 12 or 18 elements in axial direction. The polynomial order is varied between $N=8$ and $N=16$. The velocities are (now) normalized with ν/D. The cylinder is of the finite height $H=8D$. The endplates are chosen to be stress free to prevent deformations due to otherwise appearing Ekman layers. This kind of boundary conditions has no influence on the instability itself. Without endplate effects, the data analysis is easier and the height of the cylinder can be less than with solid endplates. For a real experiment, one needs to take this into account.

The applied external field with $\mu_B=1$ becomes unstable if the Hartmann number is large enough (cf. Fig. 1). The mode $m=1$ is the only linearly unstable mode so that higher m only appear as a result of nonlinear interactions. The spectrum becomes rather steep. While the energy of the $m=1$ mode is about 1% of that of the external field (the $m=2$ mode contains 0.08%), the energy of the mode with $m=6$ is already four orders of magnitude less than that of $m=1$.

In the rotating case with Re$=500$ after about 50 rotations, a steady state is reached. Figure 2 shows the resulting pattern of the axial EMF for a simulation of the instability with Ha$=200$ for the small magnetic Prandtl number Pm$=0.01$. The EMF is given in the dimensionless units $\nu B_{\rm in}/D$, it is negative everywhere. The cells prove to be rather flat for Pm of order unity. The EMF ($\simeq 100$) averaged over the whole container is plotted in Fig. 3 as a dot at Pm$=0.01$.

From Fig. 3, one finds that for various Pm the averaged EMF runs as E/Pm with $E\simeq 1.2$. The resulting EMF in physical units is therefore

$$\mathcal{E}_z = -E\eta\frac{B_{\rm in}}{D}, \tag{13}$$

which does not depend on the molecular viscosity ν. The magnetic Prandtl number does not play any role in this expression. This is our chance to work in experiments also with conducting fluids with small magnetic Prandtl numbers.

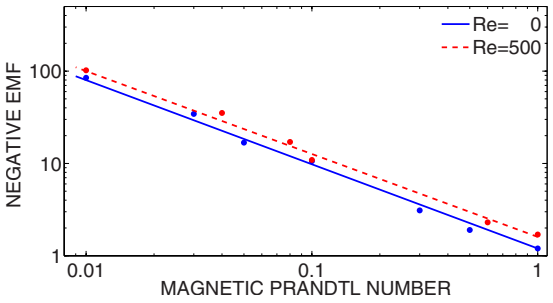

FIG. 3. (Color online) The negative normalized axial EMF vs Pm for Ha$=200$ and for $\mu_B=1$ averaged over the container. The lower curve is from simulations without rotation; the upper curve with rotation and shear (Re$=500$, $\mu_\Omega=0.35$).

A negative EMF leads to positive $\eta_{\rm T}$. From Eqs. (12) and (13) follows:

$$\frac{\eta_{\rm T}}{\eta} \simeq 1.5E \simeq 1.8 \tag{14}$$

for resting cylinders and for all Pm. The voltage difference δU due to this EMF becomes $\delta U = E\eta B_{\rm in}H/D$ with H as the container height. Transition to the Hartmann number yields

$$\delta U = E\eta\sqrt{\mu_0\rho\nu\eta}\frac{H}{D^2}\mathrm{Ha}. \tag{15}$$

For $D=10$ cm, $H=100$ cm, and for sodium ($\sqrt{\mu_0\rho\nu\eta} \simeq 8.15$) a maximum value of 16 mV as the potential difference from endplate to endplate results. This value bases on the scaling with $1/\mathrm{Pm}$ suggested by Fig. 3 and must thus be considered as an estimation. Even in the case, however, that the slope of the curve decreases for smaller Pm, the effect should be observable in the laboratory.

To reach a Hartmann number of 200, a magnetic field of 163 G at the inner cylinder ($R_{\rm in}=10$ cm) is required, which can be produced with an axial current of 8.15 kA for $R_{\rm out}=2R_{\rm in}$.

Note that the resulting potential difference runs with $1/D^2$ so that for containers with smaller gaps the resulting value strongly increases. For a gap of only 1 cm (but still $\hat{\eta}=0.5$!), the potential difference approaches 1.6 V.

For studies of the rotational influence on the TI, also the theoretical EMF under the presence of a differential rotation, are given in Fig. 4. It is $\mu_\Omega=0.35$ (quasi-Kepler flow), and the Reynolds number is Re$=500$. Note that the influence of the rotation is only weak; with rotation, the values are slightly higher than without rotation ($\eta_{\rm T}/\eta \simeq 2.4$). This is understandable as after Fig. 1 for Re$=500$ a differential rotation with $\mu_\Omega < 0.45$ destabilizes the magnetic field. More flat rotation laws with $\mu_\Omega \gtrsim 0.45$ lead to the opposite result. There is no indication that our basic result (13) is modified by such rotation laws.

Figure 4 gives the values of $\eta_{\rm T}/\eta$ resulting from simulations with various magnetic Prandtl numbers Pm. Even for the case that the very weak trend to smaller values for

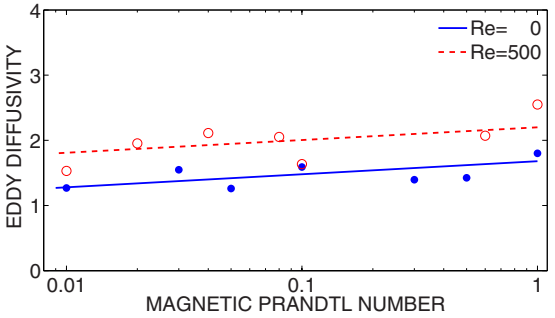

FIG. 4. (Color online) The ratio η_T/η vs Pm for Ha=200 and μ_B=1. The lower curve is without rotation; the upper curve is with rotation and shear (Re=500, μ_Ω=0.35).

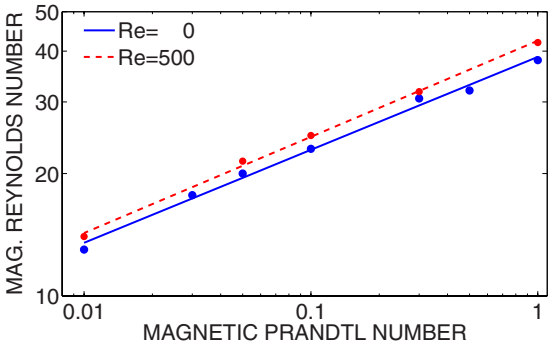

FIG. 5. (Color online) The same as in Fig. 4 but for the magnetic Reynolds number Rm′ of the fluctuations.

smaller Pm is real, the estimated value of η_T/η for sodium or gallium should be much higher than (say) 10%.

Next the magnetic Reynolds number of the fluctuations,

$$\mathrm{Rm}' = \frac{\max(\sqrt{\langle u'^2\rangle})D}{\eta}, \tag{16}$$

is considered. Only a very weak magnetic Prandtl number dependence of Rm′ is found (Fig. 5). Extrapolation of the results to Pm=10^{-5} gives a value of Rm′ $\simeq$ 2.6 without and with rotation. The corresponding velocity fluctuations for sodium are about 1.5 m/s in a gap of 10 cm. The values are rather similar to those of the Riga "α-yashchik" experiment [19]. Even with two resting cylinders, it is possible to produce rather high (azimuthal) velocities in TI experiments.

V. CONCLUSIONS

We have shown by numerical simulations that the nonaxisymmetric Tayler instability for nearly homogeneous toroidal fields in cylindric TC containers produces an axial value of the EMF, which is almost independent of the fluid's viscosity. From numerical reasons, the magnetic Prandtl numbers only covered the range between 0.01 and 1. Hence, if extrapolation to fluids with small magnetic Prandtl numbers is allowed, liquid metals can be used to find this EMF in experiments. The resulting EMF for a container with 10-cm-gap width equals 16 mV/m corresponding to an eddy diffusivity of η_T on the order of the microscopic diffusivity η. This value essentially exceeds the numbers observed in other existing experiments. We did not find a remarkable influence of differential rotation between the cylinders on the EMF. The concept of the proposed experiment can thus further be developed to simultaneous measurements of the eddy viscosity and, therefore, the magnetic Prandtl number.

Also the magnetic Reynolds number of the fluctuations exhibits rather slight dependencies on both the fluid's viscosity and the basic rotation (Fig. 5). Interpolation to smaller Pm leads for sodium to fluctuations of the azimuthal velocity of about 1 m/s. For smaller gaps, the velocities are even higher.

With an inner radius of 10 cm, the magnetic field in the gap is on the order 100 G. It can be produced by a system of electric currents. For the favored almost uniform radial profile of the magnetic, the currents along the axis of the container and through the sodium are parallel and of the same amplitude of about 6 kA (19 kA for gallium). Magnetic fields increasing outward (e.g., by a factor of 2) are much more unstable so that the necessary electric currents are reduced (see Table I).

[1] R. J. Tayler, Proc. Phys. Soc. London, Sect. B **70**, 31 (1957).
[2] Yu. V. Vandakurov, SvA **16**, 265 (1972).
[3] R. J. Tayler, Mon. Not. R. Astron. Soc. **161**, 365 (1973).
[4] J. Braithwaite, Astron. Astrophys. **449**, 451 (2006).
[5] M. Gellert, G. Rüdiger, and D. Elstner, Astron. Astrophys. **479**, L33 (2008).
[6] A. B. Reighard and M. R. Brown, Phys. Rev. Lett. **86**, 2794 (2001).
[7] P. Frick, S. Denisov, V. Noskov, and R. Stepanov, Astron. Nachr. **329**, 706 (2008).
[8] R. Monchaux *et al.*, Phys. Rev. Lett. **98**, 044502 (2007).
[9] D. H. Michael, Mathematika **1**, 54 (1954).
[10] E. P. Velikhov, Sov. Phys. JETP **9**, 995 (1959).
[11] G. Rüdiger, M. Schultz, D. Shalybkov, and R. Hollerbach, Phys. Rev. E **76**, 056309 (2007).
[12] E. Pitts and R. J. Tayler, Mon. Not. R. Astron. Soc. **216**, 139 (1985).
[13] G. Rüdiger, R. Hollerbach, M. Schultz, and D. Elstner, Mon. Not. R. Astron. Soc. **377**, 1481 (2007).
[14] D. Shalybkov, Phys. Rev. E **73**, 016302 (2006).
[15] S. I. Vainshtein and L. L. Kichatinov, Geophys. Astrophys. Fluid Dyn. **24**, 273 (1983).
[16] T. A. Yousef, A. Brandenburg, and G. Rüdiger, Astron. Astrophys. **411**, 321 (2003).
[17] M. Gellert, G. Rüdiger, and A. Fournier, Astron. Nachr. **328**, 1162 (2007).
[18] M. O. Deville, P. F. Fischer, and E. H. Mund, *High-Order Methods for Incompressible Fluid Flow* (Cambridge University Press, Cambridge, 2002).
[19] F. Krause and K.-H. Rädler, *Mean-Field Magnetohydrodynamics and Dynamo Theory* (Akademie-Verlag, Berlin, 1980).